RSC Advances

RSC Publishing

PAPER

View Article Online
View Journal | View Issue

Cite this: *RSC Advances*, 2013, **3**, 15185

Triborate and pentaborate salts of non-metal cations derived from *N*-substituted piperazines: synthesis, structural (XRD) and thermal properties†

Michael A. Beckett,*[a] Peter N. Horton,[b] Michael B. Hursthouse[b] and James L. Timmis[a]

Received 15th May 2013,
Accepted 6th June 2013

DOI: 10.1039/c3ra42387e

www.rsc.org/advances

The synthesis and characterization of a triborate salt, $[H_2N(CH_2CH_2)_2NH_2][B_3O_3(OH)_4]_2$ (**1**), and four pentaborate salts, $[H_2N(CH_2CH_2)_2NH][B_5O_6(OH)_4]$ (**2a**), $[MeHN(CH_2CH_2)_2NH][B_5O_6(OH)_4]$ (**2b**), $[MeHN(CH_2CH_2)_2NMe][B_5O_6(OH)_4]$ (**2c**) and $[Me_2N(CH_2CH_2)_2NMe_2][B_5O_6(OH)_4]_2$ (**2d**) are described. TGA and DSC analysis (in air, 25–1000 °C) indicate that triborate **1** decomposes to B_2O_3 *via* a multistage process, with the first stage (<250 °C) being dehydration to condensed polymeric hexaborate of approximate composition: $[H_2N(CH_2CH_2)_2NH_2][B_6O_{10}]$. The pentaborates (**2a–2d**) are thermally decomposed to B_2O_3 *via* a 2 stage process involving polymeric $[NMC][B_5O_8]$. The anhydrous polyborates were amorphous. BET analysis of materials derived from the thermolysis of **1** at 250, 400, 600, and 1000 °C, were all non-porous (surface area <1.8 $m^2\ g^{-1}$). A single-crystal X-ray diffraction study of **1** showed that it contains isolated triborate(1−) anions in a structure comprised of alternating cationic and anionic layers held together *via* extensive H-bonds. Single-crystal XRD structural studies on pentaborate salts **2c** and **2d** are also reported.

1. Introduction

There has been increased interest in recent years in non-metal cation (NMC) polyborate, notably pentaborate, salts as a result of their potential applications as porous[1–5] or NLO[6] piezoelectric[7] or fluorescent[8] materials. The chemistry of boric acid in aqueous solution is complicated with monomeric and various polymeric borate ions existing in equilibrium concentrations[9] which are dependent upon B concentration, $B/[OH^-]$ ratio, and temperature. Despite this, pentaborate salts of NMCs are generally readily synthesized as crystalline solids from aqueous solution by the interaction of a free base, or its hydroxide salt, with $B(OH)_3$ in a 1 : 5 ratio.[2,4,10] Structurally, NMC pentaborates are best described as supramolecular networks of H-bonded isolated $[B_5O_6(OH)_4]^-$ anions, and the formation of this extended lattice is clearly a driving force in product formation. The NMCs occupy 'cavities' within the network, and usually (if possible) add further stabilizing H-bond cation-anion interactions.[1,2,4] Occasionally, NMC polyborate salts other than pentaborates have been obtained from aqueous solution *e.g.* $[B_3O_3(OH)_4]^-$,[11] $[B_4O_5(OH)_4]^{2-}$,[12] $[B_7O_9(OH)_5]^{2-}$ (2 isomers),[13,14] $[B_8O_{10}(OH)_6]^{2-}$,[2] $[B_9O_{12}(OH)_6]^{2-}$,[15,16] $[B_{14}O_{20}(OH)_6]^{4-}$.[17] More forcing solvothermal methods have led to NMC salts of isolated or condensed polyborate sheets, which are formally derived from isolated anions.[18] We are currently undergoing a research programme investigating the structure directing effects of NMCs in borate chemistry[4,14,19] and have recently isolated, by this method from aqueous solution,[20] an unprecedented double salt of stoichiometry $[H_2en]_2[B_{11}O_{18}(OH)]\cdot 7H_2O$ which contains two isolated polyborate anions: $[B_4O_5(OH)_4]^{2-}$ and $[B_7O_9(OH)_5]^{2-}$. As a continuation of this study we have investigated substituted piperazine based NMCs and now report the synthesis of an unusual triborate salt, as well as further examples of pentaborate salts. The structures of the anions present are illustrated in Fig. 1. The thermal properties of the triborate salt (TGA/DSC) has been investigated in detail and results compared with those of the pentaborate derivatives. Porosity (BET surface area measurements) of materials derived from the thermal decomposition of the triborate salt are also

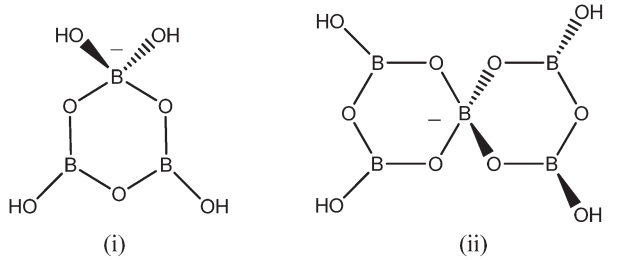

Fig. 1 Schematic drawing of (i) triborate(1−) as observed in **1**, and (ii) pentaborate(1−) as observed in **2a–2d**.

[a]*School of Chemistry, Bangor University, Bangor, Gwynedd, LL57 2UW, UK. E-mail: m.a.beckett@bangor.ac.uk; Fax: +44(0)1248 382734; Tel: +44(0) 1248 37*
[b]*School of Chemistry, University of Southampton, Southampton, SO17 1BJ, UK*

† Electronic supplementary information (ESI) available. For crystallographic data in CIF or other electronic format see DOI: 10.1039/c3ra42387e

described. These results are compared with those from other known NMC polyborate salts.

2. Results and discussion

2.1 Synthesis and characterization

The triborate salt $[H_2N(CH_2CH_2)_2NH_2][B_3O_3(OH)_4]_2$ (**1**), and the pentaborate salts $[H_2N(CH_2CH_2)_2NH][B_5O_6(OH)_4]$ (**2a**), $[MeHN(CH_2CH_2)_2NH][B_5O_6(OH)_4]$ (**2b**), and $[MeHN(CH_2CH_2)_2NMe][B_5O_6(OH)_4]$ (**2c**) were conveniently prepared in H_2O/MeOH solution, from $B(OH)_3$ and (substituted) piperazines according to eqn (1) and (2).

$[Me_2N(CH_2CH_2)_2NMe_2][B_5O_6(OH)_4]_2$ (**2d**) was prepared by reacting a solution of $[Me_2N(CH_2CH_2)_2NMe_2][OH]_2$, which were obtained from ion exchange of the diiodide salt, with $B(OH)_3$ as shown in eqn (3). Eqn (1) and (2) indicate that a piperazine : $B(OH)_3$ ratio of 1 : 6 would be ideal for the preparation of **1**, whereas a similar 1 : 5 ratio would be ideal for **2a**. We obtained **1** in high yield from a 1 : 3 ratio reaction mixture in which half of the piperazine remained unreacted. We believe the function of the unreacted piperazine is to raise pH of the solution allowing the more basic triborate anion[5,15] to crystallize.

$$[HN(CH_2CH_2)_2NH] + 6B(OH)_3 \rightarrow [H_2N(CH_2CH_2)_2NH_2][B_3O_3(OH)_4]_2\ (\mathbf{1}) + 4H_2O \quad (1)$$

$$[RN(CH_2CH_2)_2NR'] + 5B(OH)_3 \rightarrow [RNH(CH_2CH_2)_2NR'][B_5O_6(OH)_4] + 5H_2O\ (R = R' = H,\ (\mathbf{2a});\ R = Me,\ R' = H,\ (\mathbf{2b});\ R = R' = Me,\ (\mathbf{2c})) \quad (2)$$

$$[Me_2N(CH_2CH_2)_2NMe_2][OH]_2 + 10B(OH)_3 \rightarrow [Me_2N(CH_2CH_2)_2NMe_2][B_5O_6(OH)_4]_2\ (\mathbf{2d}) + 12H_2O \quad (3)$$

With the exception of **2d** (obtained in 50%) products were readily obtained in high yield (86–97%) and were of good analytical purity by crystallization induced by removal of the solvents. Compounds **1** and **2a–d** were characterized spectroscopically (NMR, IR) and X-ray diffraction (powder) techniques. Powder diffraction analysis showed that all samples were prepared crystalline, and crystals from **1**, **2c** and **2d** were selected for a single-crystal structural determination (section 2.4). Unsubstituted piperazine salts usually contain dications, with monocationic salts occurring less frequently.[21] ^{11}B NMR spectra of salts **1** and **2a–d** are all very similar, despite the different stoichiometry for **1**, and showed peaks at +18 ppm, +13 ppm and +1 ppm. The similarity in these spectra may be explained by the existence of a complex series of equilibria existing in aqueous solution which link monomeric and oligomeric borate species.[9] Similar spectra have been obtained from other pentaborate salts.[4,14,19] ^{1}H and ^{13}C NMR spectra, obtained in D_2O solution, were in full accord with their structures, with signals associated with B–OH and NH protons producing a single broadened single at ~4.7 ppm due to rapid exchange. The IR spectrum of **1** (Fig. 2) displayed strong B–O peaks at 1414 cm^{-1}, 1305 cm^{-1}, 985 cm^{-1} and 862 cm^{-1} which may be assigned by reference to Li *et al.*[22] to $\nu_{as}(B_{(3)}–O)$, $\nu_{as}(B_{(3)}–O)$, $\nu_{s}(B_{(3)}–O)$ and $\nu_{s}(B_{(4)}–O)$, respectively. The strong

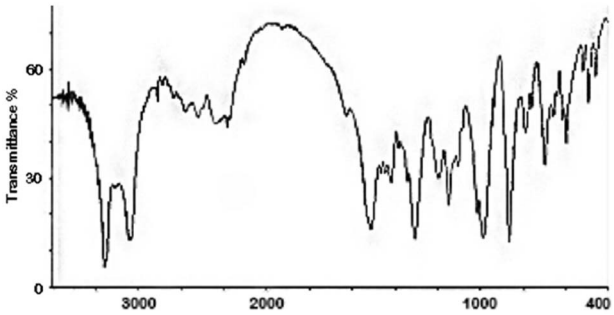

Fig. 2 IR spectrum of the triborate salt for **1**.

peak at 1510 cm^{-1} may be an NH or OH bending vibration. The diagnostic[23] $\nu_{s}(B_{(3)}–O)$[22] band at ~925 cm^{-1} is apparent in the pentaborate samples **2a–d**, but significantly is absent from **1**.

2.2 Thermal properties of 1

The thermal properties of NMC pentaborate salts, which contain intricate 3D H-bonded networks (section 2.3), have been well investigated and the thermal behaviour of **2a–2d** are consistent with earlier reports on pentaborate salts.[1–5] The layered structure for **1** (see section 2.3) might suggest that its thermal properties would be different and therefore was worthy of further and more detailed investigation.

Heating a sample of the triborate salt (**1**) in air resulted in thermal decomposition and the eventual formation of a glassy black solid. During this process the sample 'chars' and intumesces prior to collapsing down to the glass. This behaviour is similar to that observed for non-metal cation pentaborates.[1–5] A thermal study of the one previously known NMC triborate, $[HOCH_2CMe_2NH_3][B_3O_3(OH)_4]$,[11] suggested dehydration (2 mole equivalent per triborate) by 120 °C to a viscous liquid by either condensation of anions or anion/cation esterification. The process for **1** was followed in more detail by DSC/TGA (Fig. 3). Closer inspection of the TGA curve shows that the decomposition is a multistep process, with a series of endothermic processes occurring below 275 °C, and two exothermic processes occurring at 400 °C and 600 °C. The weight loss below 275 °C is consistent with dehydration as

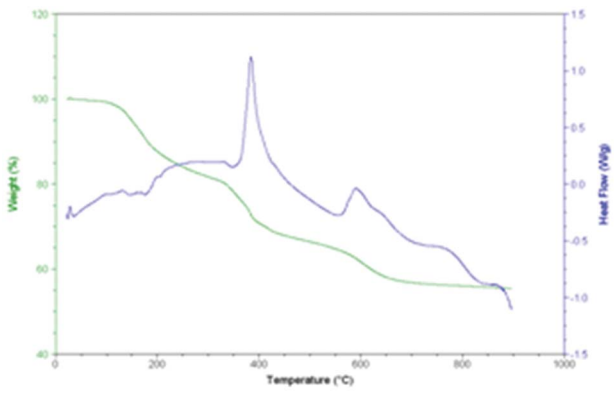

Fig. 3 TGA/DSC trace for **1**.

shown in eqn (4). The final residue (55.4%) is in close agreement with that calculated (54.2%) for B_2O_3 according to eqn (5).

$$[H_2N(CH_2CH_2)_2NH_2][B_3O_3(OH)_4]_2 \rightarrow [H_2N(CH_2CH_2)_2NH_2][B_6O_{10}] + 4H_2O \quad (4)$$

$$[H_2N(CH_2CH_2)_2NH_2][B_3O_3(OH)_4]_2 \rightarrow 3B_2O_3 + \text{oxidation products} \quad (5)$$

It was of interest to examine the physical properties (crystallinity and porosity) of materials derived from the aerobic thermolysis of **1** and a furnace procedure was used to attempt to replicate the above TGA results on a small synthetic scale. Accordingly, samples (~1.0 g) were heated to 275 °C (**1a**), 500 °C (**1b**), 600 °C (**1c**), or 1000 °C (**1d**) and weighed and characterized. Elemental analytical data of **1a** were consistent with the dehydrated product (eqn (4)) and the residual weight associated with formation of **1d** was in good agreement with the residual weight calculated expected for formation of B_2O_3. Elemental analysis data for **1b** and **1c** demonstrated residual presence of C, H and N with lower amounts present in **1c** indicating that the oxidation process was still incomplete at this temperature/time. All thermally produced samples were amorphous by powder XRD studies. and SEM pictures of ground samples were all remarkably similar (exemplified for **1b** in Fig. 4) and were consistent with glassy shards.

The porosity of the thermally derived materials were determined by multipoint BET analysis.[24] Essentially all samples were 'non-porous' with the isolated pentaborates having porosities of 0.12–0.85 $m^2\ g^{-1}$, condensed pentaborates 0.04–0.86 $m^2\ g^{-1}$, intumesced materials 0.12–1.59 $m^2\ g^{-1}$, and the final glassy B_2O_3, 0.18 $m^2\ g^{-1}$. The densities of **1b** and **1c**, determined as 'tipped solids', were extremely low (0.1, 0.2 g cm^{-3} respectively) and are consistent with the observation that the materials intumesced during oxidation to leave expanded materials. The low porosity of the final glassy black solid

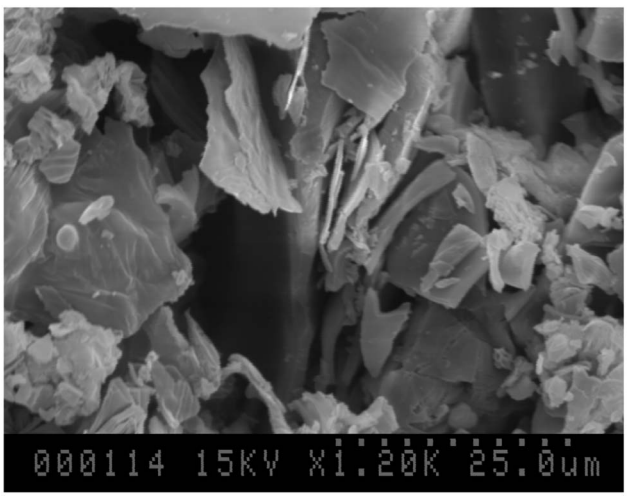

Fig. 4 SEM of **1b** (sample **1** calcined at 500 °C, 24 h) having been ground in a mortar and pestle.

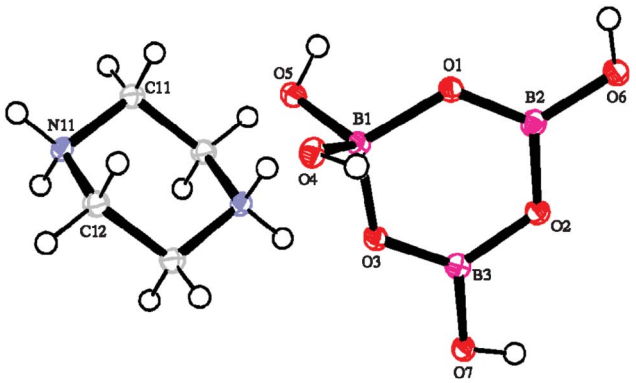

Fig. 5 ORTEP drawing of ions present in $[H_2N(CH_2CH_2)_2NH_2][B_3O_3(OH)_4]_2$ (**1**) showing atomic numbering scheme. Selected bond distances (Å) and angles (°) for $[B_3O_3(OH)_4]^-$ anion: B1–O4, 1.453(2); B1–O5 1.456(2); B1–O3 1.486(2); B1–O1 1.497(2); B2–O1 1.351(2); B2–O6 1.359(2); B2–O2 1.400(2); B3–O3 1.337(2); B3–O7 1.378(2); B3–O2 1.396(2). O1–B1–O3 110.16(13); B1–O1–B2 124.38(13); O1–B2–O2 120.59(15); B2–O2–B3 118.72(13); O2–B3–O3 122.39(15); B3–O3–B1 123.69(13).

(~B_2O_3) was expected, but the porosity of the intumesced materials were lower than expected and indicated macroporous aerogel-like structures, in which gaseous decomposition products were trapped within the intumesced materials.[25]

2.3 XRD structural studies on 1, 2c and 2d

The structure of **1** as a triborate salt of a dication was confirmed by single-crystal XRD studies. A drawing of **1** showing the ions present and the atomic numbering scheme is shown in Fig. 5. The structure contains two identical $[B_3O_3(OH)_4]^-$ anions, as illustrated in Fig. 1(i), partnered by one $[H_2N(CH_2CH_2)_2NH_2]^{2+}$ cation which adopts the familiar chair conformation.[26] The $[B_3O_3(OH)_4]^-$ anion appears in significant concentrations in aqueous solution at pH 5–12 but rarely is crystalized from such solutions by non-metal cations which generally favour partnering pentaborate anions. As noted above, the solutions had excess base present, and the pH was higher than normal.[5,15] Structurally characterized triborate(1-) salts are uncommon and are limited to two alkali metal salts $Na[B_3O_3(OH)_4]$ (ref. 27) and $K[B_3O_3(OH)_4]\cdot H_2O$,[28] and a NMC salt $[HOCH_2C(Me)_2NH_3][B_3O_3(OH)_4]$.[11] Interatomic distances and angles for the triborate anion of **1** are given in the caption to Fig. 5. The B_3O_3 ring in **1** deviates slightly from planarity and adopts an envelope conformation with 4-coordinate B1 0.034 Å from the plane containing B2B3O1O3. O2 is 0.008 Å below the same plane but this distance is not significant. Similar ring conformations are found for $Na[B_3O_3(OH)_4]$ (ref. 27) and $K[B_3O_3(OH)_4]\cdot H_2O$.[28] The anion in $[HOCH_2C(Me)_2NH_3][B_3O_3(OH)_4]$ (ref. 11) adopts a half-chair conformation with the 4-coordinate B 0.206 Å out of the plane containing the 3 ring O atoms. The bond lengths and bond angles for **1** are not significantly different from those found for $[HOCH_2C(Me)_2NH_3][B_3O_3(OH)_4]$ (ref. 11) with O–B_{tetra} significantly longer than O–B_{trig} and vary systematically about the ring, as has been observed or related organotriboroxine adducts[29] and organotriboroxinates,[30] with B2–O1 and B3–O3 being significantly shorter.

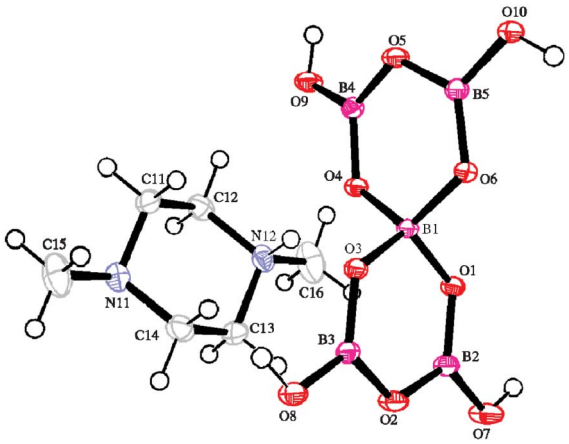

Fig. 6 ORTEP drawing of ions present in $[MeHN(CH_2CH_2)_2NMe][B_5O_6(OH)_4]$ (**2c**) showing atomic numbering scheme.

Compound **1** has a giant H-bonded network involving both anion-anion and cation-anion interactions and where all four NH and all four OH groups participate as donors. For convenience, the O atom acceptor sites in **1** may be labelled, by analogy with pentaborate chemistry and distance from the 4 co-ordinate B1, α-, β- or γ-sites.[2] The OH sites on B1 can be labelled δ. The triborate anions form infinite zig-zag chains through alternating γ and α $R_2^2(8)$ rings (Etter[31]). The D···A distances/angle at H for the α and γ interactions are 2.7453(16) Å/176.4° and 2.7179(16) Å/167.0°, respectively. These chains are then stacked into layers by H-bond interactions from the two OH groups on B1 to β-sites as C(6) interactions with D···A distances/angle at H of 2.8312(17) Å/162.8° and 2.8258(16) Å/169.5°. The layers are separated by layers of $[H_2N(CH_2CH_2)_2NH_2]^{2+}$ cations which are H-bonded to δ acceptor sites of the triborate anion *via* unusual $R_3^3(10)$ rings. The D···A distances/angle at H for the cation–anion interactions are 2.7182(18) Å/165.0° and 2.6786(18) Å/163.3°.

The structures of **2c** and **2d** were confirmed by single crystal XRD studies. Drawings of **2c** and **2d** are shown in Fig. 6 and 7,

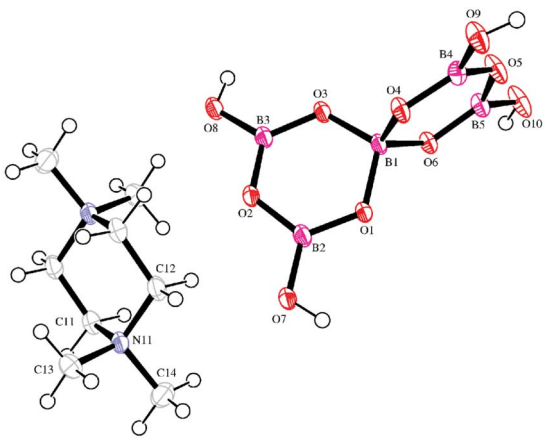

Fig. 7 ORTEP drawing of ions present in $[Me_2N(CH_2CH_2)_2NMe_2][B_5O_6(OH)_4]_2$ (**2d**) showing atomic numbering scheme.

respectively. Both compounds contain isolated $[B_5O_6(OH)_4]^-$ anions, as illustrated in Fig. 1(ii). B–O bond lengths and bond angles at B and O are not significantly different from those observed in other pentaborate structures containing non-metal cations, and related systems.[1–4,14,19,32]

The anions in both compounds form remarkably similar (despite the stoichiometry) extended H-bonded lattices, and the H-bond interactions for both **2c** and **2d** can be described as α,α,α,β. The α,α,α,β configuration is commonly found in 'brickwall' or 'herringbone' structures[1,14] but the extended lattice found in **2c** and **2d** is not one of these types. Each pentaborate anion forms 3 reciprocal-pair $R_2^2(8)$ α-interactions with neighboring pentaborates, and 1 reciprocal-pair $R_2^2(12)$ β-interaction (Etter[31]). The $R_2^2(12)$ has not been previously observed in pentaborate systems and is responsible for the unusual extended lattices in **2c** and **2d**. The D···A distances/angle at H for these β interactions in **2c** and **2d** are 2.8508(10) Å/165.0° and 2.8182(19) Å/178.2°, respectively. Compound **2c** has an additional H-bond contact between the cation and the α-position of a pentaborate (N12–H12···O4) with a N···O distance of 2.7548(11) Å and NHO angle of 169.2°.

3. Experimental

3.1 General

Reagents were purchased from Aldrich Chemical company and used without purification. Multi-element NMR spectra were recorded at room temperature (298 K) on a Bruker Avance 500 (11.7 T) spectrometer operating at 500 MHz for ^1H, 125 MHz for ^{13}C–{^1H}, and 160 MHz for ^{11}B–{^1H} and referenced to $SiMe_4$ or $BF_3{\cdot}OEt_2$ using D_2O as solvent. Chemical shifts (δ) are reported in ppm. Elemental analyses were performed at OEA Laboratories Ltd (Callington, UK). Powder XRD data were obtained on a Philips 1050/37 X-ray diffractometer, equipped with an iron filter, using Cu-Kα radiation (λ = 0.154056 nm) with a continuous scan between the range 2θ = 5–75°. Philips X'Pert System software was used to collect and manipulate the data. TGA and DSC analyses were obtained using a Netzch TG 209 instrument. BET multipoint analyses were performed on a Micromeritics Gemini III 2375 instrument.

3.2 Synthesis of $[H_2N(CH_2CH_2)_2NH_2][B_3O_3(OH)_4]_2$ (1)

$B(OH)_3$ (4.31 g, 69.67 mmol) was dissolved in 50 : 50 H_2O/MeOH (100 ml) with gentle warming. To this solution was added piperazine (2.00 g, 23.25 mmol) with stirring, and the solution was gently warmed (50 °C) for 1 h. The majority of the solvent (H_2O/MeOH) was removed under reduced pressure (rotary evaporator), and the remaining solid, obtained by filtration, was placed in an oven to dry for 4 h at 100 °C. The product **1** was obtained as a white crystalline solid was obtained 4.5 g, (97%). Crystals were analytically pure and were suitable for X-ray diffraction studies. Elem. anal. ($C_4H_{20}B_6N_2O_{14}$). Calc: C 12.5, H 5.2, N 7.3%; Found: C 12.7, H 5.3, N 7.1%. Mpt > 260 °C (dec). NMR: δ_H/ppm 2.96 (8H, s), 4.7 (12H). δ_C/ppm 42.4 ($4CH_2$). δ_B/ppm 1.1 (5%), 13.2 (20%) 18.8 (75%) ν_{max}/cm^{-1} 3511(s), 3265(s), 1509(s), 1414(m), 1303(s), 1193(m), 1146(m), 985(s), 862(s), 696(m), 596(m).

XRD: d-spacing/Å (% rel. int.): 3.49 (100), 5.45 (81), 2.63 (78), 4.22 (71), 5.51 (53), 3.70 (37).

3.3 Synthesis of [NMC][$B_5O_6(OH)_4$)] (2a–2d)

A similar procedure to that detailed in section 3.2 was used for **2a–c** but with a $B(OH)_3$ ratio of 5 : 1.

2a. From $B(OH)_3$ (7.02 g, 113.6 mmol) and piperazine (2.00 g, 23.25 mmol). 5.84 g (86%). Elem anal. ($C_4H_{15}B_5N_2O_{10}$). Calc: C 15.7, H 4.9, N 9.2%; Found: C 14.3, H 5.4, N 8.9%. Mpt. 260 °C (dec). NMR: δ_H/ppm 2.95 (8H, s), 4.7 (7H). δ_C/ppm 42.47. δ_B/ppm 0.8 (15%), 12.0 (25%), 17.3 (60%). XRD: d-spacing/Å (% rel. int.): 3.50 (100), 3.72 (99), 5.55 (44), 7.00 (29), 3.30 (27), 4.25 (24).

2b. From $B(OH)_3$ (6.18 g, 100.0 mmol) and *N*-methylpiperazine (2.00 g, 20.00 mmol). 5.78 g (91%). Elem anal. ($C_5H_{17}B_5N_2O_{10}$). Calc: C 18.8, H 5.7, N 8.8%; Found: C 18.6, H 5.4, N 8.5%. Mpt > 260 °C (dec). NMR: δ_H/ppm 2.29 (3H, s), 2.68 (4H, s), 3.08 (4H) 4.7 (6H). δ_C/ppm 42.9 ($2CH_2$), 44.3 (CH_3), 51.2 ($2CH_2$). δ_B/ppm 1.0 (5%), 12.5 (20%), 17.5 (75%). ν_{max}/cm^{-1} 3380(s), 3054(s), 1431(s), 1362(s), 1252(m), 1162(m), 1101(m), 925(s), 782(m), 697(m), 591(m), 465(m). XRD: d-spacing/Å (% rel. int.): 3.71 (100), 4.84 (66), 3.45 (65), 7.33 (30), 2.76 (29), 3.50 (27).

2c. From $B(OH)_3$ (5.41 g, 87.7 mmol) and *N*,*N*′-dimethylpiperazine (2.00 g, 17.5 mmol). 5.35 g, 92%). Elem anal. ($C_6H_{19}B_5N_2O_{10}$). Calc: C 21.5, H 6.3, N 8.4%; Found: C 20.9, H 5.7, N 7.9%. Mpt. 260 °C (dec). NMR: δ_H/ppm 2.45 (6H, s), 2.85 (8H, s), 4.70 (5H, s). δ_C/ppm 43.5 ($4CH_2$), 52.3 ($2CH_3$). δ_B/ppm 1.2 (15%, s), 13.3 (25%, s), 18.5 (60%, s). ν_{max}/cm^{-1} 3313(s), 3035(m), 2810(m), 1433(s), 1308(s), 1192(m), 1142(m), 1025(s), 926(s), 774(m), 709(m), 471(m). XRD: d-spacing/Å (% rel. int.): 5.73 (100), 3.60 (96), 4.17 (88), 2.94 (84), 4.14 (84), 6.21 (49), 3.83 (28).

2d. *N*,*N*,*N*′,*N*′-tetreamethylpiperazinium(2+) diodide (4.0 g, 10.00 mmol) was dissolved in H_2O (50 ml) and Dowex 550A monosphere (OH^- form) was added and stirred for 24 h. The ion exchange resin was removed by filtration and MeOH (50 ml) was added to the filtrate. $B(OH)_3$ (3.09 g, 50.0 mmol) was added and the solution was heated for 1 h. The solvent was removed on a rotary evaporator to yield a white solid (3.08, 50%). Elem anal. ($C_8H_{28}B_{10}N_2O_{20}$). Calc: C 16.6, H 4.9, N 4.8%; Found: C 17.1, H 5.8, N 2.4%. Mpt > 260 °C (dec).

NMR: δ_H/ppm 3.60 (12H, s), 3.88 (8H, s). 4.70 (4H, s). δ_C/ppm 30.2 ($4CH_3$), 55.5 ($8CH_2$).δ_B/ppm 1.2 (15%), 13.5 (25%), 18.9 (60%). ν_{max}/cm^{-1} 3386(s), 1409(s), 1321(s), 1201(m), 1142(m), 1040(s), 930(s), 868(s), 775(m), 475(m). XRD: d-spacing/Å (% rel. int.): 5.07 (100), 5.67 (88), 3.66 (83), 4.08 (23), 3.41 (22), 6.09 (19).

3.4 Thermolysis experiments of 1

Samples of **1** were individually placed within open topped ceramic bowls and positioned within a furnace (air atmosphere). The furnace temperature was set to increase from room temperature to either 250 °C (**1a**), 500 °C (**1b**) or 600 °C (**1c**) at 10 °C per minute. After the samples had reached the required temperature they were allowed to cool to room temperature, isolated and powdered in a mortar and pestle.

Sample **1a** was pale yellow. Samples **1b** and **1c** were black and had increased their volume ~10 fold. **1a**: 0.70 g obtained from 1.02 g 74% residue; Elem anal. ($C_4H_{12}B_6N_2O_{10}$). Calc: C 15.4, H 3.9, N 8.9%; Found: C 15.1, H 4.0, N 8.6%. IR: ν_{max}/cm^{-1}: 3488(s), 3255(s), 1637(m), 1506(m), 1383(s), 1140(m), 1063(m), 864 (s), 809(m), 701(m). Density: 0.690 g cm^{-3}. BET: surface area 0.21 m^2 g^{-1}. **1b**: (0.70 g from 1.03 g, 68% residue). Elem anal. Found: C 5.3, H 2.6, N 1.9%. IR: ν_{max}/cm^{-1}: 3692(s), 3209(s), 1727(w), 1627(w), 1437(s), 1195(m), 883(w), 721(m), 644 (m), 547(w). Density: 0.096 g cm^{-3}. BET: surface area 1.90 m^2 g^{-1}. **1c**: (0.61 g from 1.02 g, 59% residue). Elem anal. Found: C 2.4, H 4.7, N 0.8%. IR: ν_{max}/cm^{-1}: 3600(m), 3220(s), 1449(s), 1196(s), 883(w), 795(m), 720(m), 644(m), 547(m). Density: 0.214 g cm^{-3}. BET: surface area 1.85 m^2 g^{-1}. In a similar experiment **1** (0.4999 g) was placed within open topped Ni crucible and positioned within the furnace (air atmo-

Table 1 Crystal data and structure refinement for **1**, **2c** and **2d**

Crystal	**1**	**2c**	**2d**
Empirical formula	$C_4H_{20}B_6N_2O_{14}$	$C_6H_{19}B_5N_2O_{10}$	$C_8H_{28}B_{10}N_2O_{20}$
Formula wt (g mol^{-1})	385.08	333.28	580.42
Crystal system, space group	Triclinic, $P\bar{1}$	Triclinic, $P\bar{1}$	Monoclinic, $P2_1/c$
a (Å)	5.7619(2)	8.8129(2)	8.1624(6)
b (Å)	6.3796(2)	8.8960(2)	11.3609(8)
c (Å)	11.6206(5)	10.3618(2)	13.7429(9)
α (°)	92.684(2)	74.043(1)	90
β (°)	98.060(2)	78.854(1)	94.416(4)
γ (°)	114.750(2)	88.962(1)	90
Vol ($Å^3$)	381.43(2)	765.80(3)	1270.63(15)
Z, Calc density (Mg m^{-3})	1, 1.676	2, 1.445	2, 1.517
μ (mm^{-1})	0.155	0.125	0.136
F(000)	200	348	600
Crystal	Colourless cut block	Colourless cut block	Colourless cut block
Crystal dimensions (mm^3)	0.08 x 0.05 x 0.03	0.28 x 0.23 x 0.18	0.42 x 0.16 x 0.10
θ range (°)	3.54–27.48	3.41–27.48	2.97–27.48
No. of reflections collected	7312	16 010	14 949
R_{int}	0.0440	0.0281	0.0486
No. of data/restraints/parameters	1746/0/122	3493/0/214	2909/0/187
Final *R* indices [$F^2 > 2\sigma(F^2)$]: R_1, wR_2	0.0416, 0.0870	0.0322, 0.0817	0.0481, 0.1194
R indices (all data): R_1, wR_2	0.0525, 0.0941	0.0358, 0.0842	0.0716, 0.1328
Largest diff. peak and hole (e $Å^{-3}$)	0.296, −0.315	0.234, −0.243	0.442, −0.298

sphere). The furnace temperature was set to increase from room temperature to 1000 °C at 10 °C per minute, and then held at 1000 °C for 3 h, and then allowed to cool to room temperature, yielding a glassy black solid (**1d**), which was powdered in a mortar and pestle and weighed (0.2759 g, 44.2% weight loss). **1d**: Elem anal. Found: C 0.1, H 0.4, N 0.1%. IR: ν_{max}/cm^{-1}: 3200(s), 1445(s), 1194(s), 795(m), 720(m), 550(m). BET: surface area 0.16 $m^2\ g^{-1}$.

3.5 X-ray crystallography

The crystallographic data collection of compounds **1**, **2c** and **2d** were performed using a Nonius Kappa CCD diffractometer with Mo-Kα radiation (λ = 0.71073 Å) controlled by the Collect[33] software package and an Oxford Cryosystem N_2 open flow cryostat at 120(2) K. The data were processed using Denzo[34] and absorption corrections were applied using SORTAV.[35] Crystallographic data are in Table 1. The structures were solved by direct methods and refined by full-matrix least-square procedures on F^2 using SHELXS-97 and SHELXL-97 respectively.[36] All non-hydrogen atoms were fixed using a standard riding model.

Crystallographic data for **1**, **2c**, **2d** have been deposited with the Cambridge Crystallographic Data Centre with CCDC 930889–930891. Copies of this information may be obtained free of charge from the Director, CCDC, 12 Union Road, Cambridge, CB2 1EZ (fax: +44 1223 336033) or email: deposit@ccdc.cam.ac.uk or www: http://www.ccdc.cam.ac.uk.

3.6 Conclusion

Salts containing cations derived from *N*-substituted piperazines, partnered with either triborate(1−) or pentaborate(1−) anions have been prepared. The triborate salt **1** possesses an alternating cationic/anionic layered solid-state structure and contains extensively H-bonded triborate sheets. Compound **1** is thermally decomposed in air *via* a multistage process to glassy B_2O_3. Materials thermally derived from **1** were amorphous and non-porous. Similar thermal behaviour was observed for the pentaborate salts (**2a–2d**) which possess three dimensional H-bonded lattices.

Acknowledgements

We thank the EPSRC for use of the X-ray crystallographic service (Southampton),[37] and Ryan Wyn-Thomas who helped with some thermolysis experiments.

Notes and references

1 (*a*) C. C. Freyhardt, M. Wiebcke, J. Felsche and G. Englehardt, *J. Inclusion Phenom. Mol. Recognit. Chem.*, 1994, **18**, 161–175; (*b*) M. Wiebcke, C. C. Freyhardt, J. Felsche and G. Englehardt, *Z. fur. Naturforsch B*, 1993, **48**, 978–985.

2 M. Z. Visi, C. B. Knobler, J. J. Owen, M. I. Khan and D. M. Schubert, *Cryst. Growth Des.*, 2006, **6**, 538–545.

3 Z.-H. Liu, J.-J. Zhang and W.-J. Zhang, *Inorg. Chim. Acta*, 2006, **359**, 519–524.

4 M. A. Beckett, P. N. Horton, M. B. Hursthouse, D. A. Knox and J. L. Timmis, *Dalton Trans.*, 2010, **39**, 3944–3951.

5 G. J. de A. A. Soler-Illa, C. Sanchez, B. Lebeau and J. Patarin, *Chem. Rev.*, 2002, **102**, 4093–4138.

6 (*a*) S. Yang, G. Li, S. Tian, F. Liao and J. Lin, *Cryst. Growth Des.*, 2007, **7**, 1246–1250; (*b*) H.-X. Liu, Y.-X. Liang and X. Jiang, *J. Solid State Chem.*, 2008, **181**, 3243–3247; (*c*) P. Becker, P. Held and L. Bohaty, *Cryst. Res. Technol.*, 2000, **35**, 1251–1262.

7 (*a*) W. R. Cook Jr. and H. Jaffe, *Acta Crystallogr.*, 1957, **10**, 705–707; (*b*) M. Touboul and E. Betourne, *Solid State Ionics*, 1993, **63**, 340–345; (*c*) A. Garja, *Phys. Status Solidi B*, 1968, **27**, K93.

8 (*a*) V. P. Dotsenko, N. P. Efryshina and I. V. Berezovskaya, *Mater. Lett.*, 1996, **28**, 517–520; (*b*) A. Akella and D. A. Keszler, *Mater. Res. Bull.*, 1995, **30**, 105–111.

9 (*a*) C. G. Salentine, *Inorg. Chem.*, 1983, **22**, 3920–3924; (*b*) J. L. Anderson, E. M. Eyring and M. P. Whittaker, *J. Phys. Chem.*, 1964, **68**, 1128–1132.

10 R. C. Petersen, M. Finkelstein and S. D. Ross, *J. Am. Chem. Soc.*, 1959, **81**, 3264–3267.

11 D. M. Schubert, M. Z. Visi and C. B. Knobler, *Inorg. Chem.*, 2008, **47**, 2017–2023.

12 (*a*) T. J. R. Weakley, *Acta Crystallogr., Sect. C: Cryst. Struct. Commun.*, 1985, **41**, 377–379; (*b*) G.-M. Wang, Y.-Q. Sun and G.-Y. Yang, *J. Solid State Chem.*, 2004, **177**, 4648–4654.

13 (*a*) C.-Y. Pan, G.-M. Wang, S.-T. Zheng and G.-Y. Yang, *Z. Anorg. Allg. Chem.*, 2007, **633**, 336–340; (*b*) D. M. Schubert, M. Z. Visi, S. Khan and C. B. Knobler, *Inorg. Chem.*, 2008, **47**, 4740–4745.

14 M. A. Beckett, P. N. Horton, M. B. Hursthouse, J. L. Timmis and K. S. Varma, *Dalton Trans.*, 2012, **41**, 4396–4403.

15 D. M. Schubert, R. A. Smith and M. Z. Visi, *Glass Technol.*, 2003, **44**, 63–70.

16 D. M. Schubert, M. Z. Visi and C. B. Knobler, *Inorg. Chem.*, 2000, **39**, 2250–2251.

17 Z.-H. Liu, L.-Q. Li and W.-J. Zhang, *Inorg. Chem.*, 2006, **45**, 1430–1432.

18 (*a*) M. Li, J.-Z. Chang, Z.-L. Wang and H.-Z. Chu, *J. Solid State Chem.*, 2006, **179**, 3265–3269; (*b*) S. Yang, G. Li, S. Tian, F. Liao, M. Xiong and J. Lin, *J. Solid State Chem.*, 2007, **180**, 2225–2232; (*c*) G.-M. Wang, C.-Y. Pan, S.-T. Zheng and G.-Y. Yang, *Acta Crystallogr., Sect. E: Struct. Rep. Online*, 2007, **63**, o1101–o1103; (*d*) G.-M. Wang, C.-Y. Pan, S.-T. Zheng and G.-Y. Yang, *Acta Crystallogr., Sect. E: Struct. Rep. Online*, 2007, **63**, o1104–o1105.

19 M. A. Beckett, C. C. Bland, P. N. Horton, M. B. Hursthouse and K. S. Varma, *J. Organomet. Chem.*, 2007, **692**, 2832–2838.

20 M. A. Beckett, P. N. Horton, S. J. Coles and D. W. Martin, *Inorg. Chem.*, 2011, **50**, 12215–12228.

21 (*a*) M. Wojtas, A. Gagor, O. Czupinski, W. Medycki and R. Jakubas, *J. Solid State Chem.*, 2012, **187**, 35–44; (*b*) G. J. Perpetuo and J. Janczak, *Acta Crystallogr., Sect. E: Struct. Rep. Online*, 2005, **E61**, o2531–o2533.

22 J. Li, S. Xia and S. Goa, *Spectrochemica Acta*, 1995, **51A**, 519, 532.

23 M. A. Beckett, P. N. Horton, S. J. Coles, D. A. Kose and A.-M. Kreuziger, *Polyhedron*, 2012, **38**, 157–161.

24 A. V. Paul and S. Natarajan, *Cryst. Growth Des.*, 2010, **10**, 765–774.

25 U. Schubert and N. Husing, *Synthesis of Inorganic Materials*, Wiley-VCH, 2nd edn, 2007, Chapter 6, pp. 305–352.
26 (*a*) S. G. Hou, *Acta Crystallogr., Sect. E: Struct. Rep. Online*, 2011, **E67**, o3292; (*b*) C. Peng, *Acta Crystallogr., Sect. E: Struct. Rep. Online*, 2011, **E67**, o2214; (*c*) S. Murugavel, R. Selvakumar, S. Godindarajan, P. S. Kannan and A. SubbiahPandi, *Acta Crystallogr., Sect. E: Struct. Rep. Online*, 2009, **E65**, o1004.
27 A. Dal Negro, J. M. Martin Pozaz and L. Ungaretti, *Am. Mineral*, 1975, **60**, 897–883.
28 C. G. Salentine, *Inorg. Chem.*, 1987, **26**, 128–132.
29 (*a*) M. A. Beckett, G. C. Strickland, K. S. Varma, D. E. Hibbs, K. M. A. Malik and M. B. Hursthouse, *J. Organomet. Chem.*, 1997, **535**, 33–41; (*b*) M. A. Beckett, G. C. Strickland, K. S. Varma, D. E. Hibbs, M. K. A. Malik and M. B. Hursthouse, *Main Group Chem.*, 1998, **2**, 251–258.
30 (*a*) M. A. Beckett, S. J. Coles, M. E. Light, L. Fischer, B. M. Stiefvater-Thomas and K. S. Varma, *Polyhedron*, 2006, **25**, 1011–1016; (*b*) M. A. Beckett, E. L. Bennett, P. N. Horton and M. B. Hursthouse, *J. Organomet. Chem.*, 2010, **695**, 1080–1083; (*c*) M. A. Beckett, C. C. Bland, P. N. Horton, M. B. Hursthouse and K. S. Varma, *Inorg. Chem.*, 2007, **46**, 3801–3803.
31 M. C. Etter, *Acc. Chem. Res.*, 1990, **23**, 120.
32 P. N. Horton, M. B. Hursthouse, M. A. Beckett and M. P. Rugen-Hankey, *Acta Crystallogr., Sect. E: Struct. Rep. Online*, 2004, **E60**, o2204–o2206.
33 R. Hooft, *Collect, Data collection software*, Nonius BV, Delft, The Netherlands, 1998.
34 Z. Otwinowski and W. Minor, *Methods Enzymol.*, 1997, **276**, 307–326.
35 (*a*) R. H. Blessing, *Acta Crystallogr., Sect. A: Found. Crystallogr.*, 1990, **A51**, 33–37; (*b*) R. H. Blessing, *J. Appl. Crystallogr.*, 1997, **30**, 421–426.
36 G. M. Sheldrick, *Acta Crystallogr., Sect. A: Found. Crystallogr.*, 2008, **A64**, 112–122.
37 S. J. Coles and P. A. Gale, *Chem. Sci.*, 2012, **3**, 683–689.